海刺猬状微纳结构钴镍化合物的合成与表征

陆春华* 陈 乐 徐 丹 倪亚茹 许仲梓
(南京工业大学材料化学工程国家重点实验室，南京 210009)

摘要：采用均相沉淀法，以 $Co(NO_3)_2 \cdot 6H_2O$ 和 $Ni(NO_3)_2 \cdot 6H_2O$ 为原料，尿素作为沉淀剂，成功制备出了新型海刺猬状微/纳复合结构。通过调节反应温度，反应物浓度和物质的量的比，所获得的前驱体呈放射状纳米线构成的海刺猬结构。随后分别在氧气氛和氢气氛下对制备出的前驱体进行热处理，利用 FE-SEM、TEM、XRD 以及 VSM 等测试手段对制备出的微/纳复合结构前驱体及热处理产物进行了形貌表征、物相分析以及磁学性能表征。在氧气氛条件下处理得到的产物具有良好的亚铁磁性，并且很好地保持了前驱体的结构与形貌。结合热处理产物的分析，对该海刺猬微纳结构前驱体提出了一种可能的形成过程和机理。另外，在氢气还原条件下处理得到的产物为多孔微纳米球状结构，呈现出更为优异的亚铁磁性。

关键词：海刺猬微纳结构；均相共沉淀；热处理；磁性能
中图分类号：O614.81+2；O614.81+3；O482.54　　**文献标识码**：A　　**文章编号**：1001-4861(2010)03-0398-07

Synthesis and Characterization of Co-Ni Compound with Urchinlike Micro/Nano Structure

LU Chun-Hua* CHEN Le XU Dan NI Ya-Ru XU Zhong-Zi
(*State Key Laboratory of Materials-Oriented Chemical Engineering, Nanjing University of Technology, Nanjing* 210009)

Abstract: Particles with urchinlike micro/nano structure were synthesized by a facile homogeneous co-precipitation process via the direct reaction between cobalt salt, nickel salt and urea. By varying the reaction temperature, concentration of reactant and reactant ratio, the obtained precursors are well-defined urchinlike particles with many thorns radially grown on the surface. After subsequent heat treatment of the corresponding precursors in oxidation and reduction atmosphere, respectively, the final products with different morphologies were characterized by FE-SEM, TEM, XRD and VSM. The heat-treated products with good ferrimagnetism fairly maintain the morphology of their corresponding precursors in oxidation atmosphere. A possible mechanism for the growth of this urchinlike architecture is proposed. It is worth noting that in reduction atmosphere, the particles grow into porous micro/nanospheres and exhibit preferable ferrimagnetism.

Key words: urchinlike micro/nano structure; homogeneous co-precipitation; heat treatment; magnetic property

0 Introduction

Much research interests have been recently focused on nanostructured magnetic materials with the expectation to control their composition, microstructure and morphology due to their wide potential applications in magnetic fluids, data storage, magnetic resonance imaging, magnetic carriers for site-specific drug delivery, etc[1-5].

Among various strategies for controlled synthesis,

收稿日期：2009-10-13。收修改稿日期：2009-12-24。
江苏省创新学者攀登项目(No.SBK200910148)，预研项目(No.51310060304)资助。
*通讯联系人。E-mail：chhlu@njut.edu.cn，Tel：+86-25-83587252
第一作者：陆春华，男，35 岁，副教授；研究方向：光电功能材料。

such as precipitation, sol-gel, micro emulsion and hydrothermal methods, many efforts have been devoted to control and tailor the morphology of the particles. Chemical synthesis has been demonstrated to be a powerful and rapid route to obtain large quantities of nanosize building blocks in a single reaction. The basic principle for chemical synthesis of nanostructured materials is to initiate chemical reactions and control the nucleation and growth of the reaction products [6]. The size, shape and composition of the magnetic nanoparticles heavily depend on the type of salts used (e.g. chlorides, sulfates, nitrates), the reactant concentration, the reaction temperature, the pH value and ionic strength of the media[7].

In recent years, nanoparticles with urchinlike morphology including ZnS [8], hollow titania spheres [9] and ZnO [10] have been successfully synthesized. These nanoparticles exhibit very interesting electrical, optical, magnetic and chemical properties, which can not be achieved by the normal nanoparticles. To date, a few examples of the preparation of magnetic nanoparticles with this morphology have been reported. Ung et al. [11] synthesized urchinlike CoNi alloy by heterogeneous nucleation using ruthenium as seeds at 170 ℃. Liu et al. [12] synthesized sea-urchin-like Ni, nickel and cobalt selenides [13] nanoparticles by hydrothermal reduction. Ma et al.[14] controllably synthesized face-centered cubic (FCC) Ni by adjusting the adding sequence of aqueous hydrazine ($N_2H_4 \cdot H_2O$), $NiCl_2$, and sodium hydroxide (NaOH) solutions.

In our present investigation, a mild and easy-manipulated method is introduced to control morphology of the nanostructured particles through treating the as-obtained precursor with desired morphologies [15]. By adjusting the reactant concentration, reaction temperature, and system of heat treatment, the morphology and structure of the final products could be easily controlled. Another concern is that the urchinlike precursors grow into porous micro/nanospheres in reduction atmosphere. To the best of our knowledge, the synthesis of these urchinlike micro/nanostructured particles has not been reported through homogeneous co-precipitation and subsequent heat treatment.

1 Experimental

1.1 Preparation of precursors

All chemical reagents were analytical grade and used without further purification. Urea was employed as the precipitator. Firstly, 0.02 mol $Co(NO_3)_2 \cdot 6H_2O$ (≥99.0%, Sinopharm Chemical Reagent Co. Ltd.), 0.01 mol $Ni(NO_3)_2 \cdot 6H_2O$ (≥98.0%, Shanghai Henxin Chemical Reagent Co. Ltd.) and 0.6 mol urea ($CO(NH_2)_2$, ≥99.0%, Guangdong Xilong Chemical Reagent Corporation) were added to distilled water (500 mL) under magnetic stirring to form homogeneous transparent solution. Secondly, the solution was transferred into an electric-heated thermostatic water bath, and heated at 75 ℃ for some time. Finally, the resulting reddish-brown precipitates were filtered, washed three times with distilled water, and then dried in an electric drying oven at 60 ℃ for 10~12 h.

1.2 Heat treatment

In a typical procedure, 1 mmol as-obtained precursor was put into a corundum crucible with capacity of 40 mL. The crucible was heated to 500 ℃ with a temperature ramp of 5 $℃ \cdot min^{-1}$ in oxidation and reduction atmosphere, respectively, and held for 2 h. The black powders were collected for characterization.

1.3 Characterization

The morphologies of the products were inspected by a LEO-1550 field emission scanning electron microscopy (FE-SEM). The transmission electron microscopy (TEM) images were taken on a JEOL2010 instrument with a tungsten filament, using an accelerating voltage of 200 kV. The sample for TEM characterization was prepared by placing a drop of sample solution on a carbon-coated copper grid and drying at room temperature. The crystalline phase was analyzed by ARL X′ TRA power X-ray diffraction system with Cu $K\alpha$ radiation source (λ=0.154 18 nm) operated at 45 kV and 35 mA, and the scan rate(2θ) of $10° \cdot min^{-1}$ was applied to record the pattern in the 2θ range of 20°~80° by means of a solid detector and a scintillation counter. Magnetic studies were carried out with a vibrating sample magnetometer (VSM) at room temperature.

2 Results and discussion

2.1 Precursors

To select an optimal reaction system to investigate the formation and properties of urchinlike micro/nano structured particles, we firstly conducted experiments to determine the parameters important for the formation of precursors with ideal urchinlike morphologies.

FE-SEM images of precursors with different concentration ratios of cobalt salt to nickel salt are shown in Fig.1. From Fig.1 one can see that the length of thorns is gradually increased with Co^{2+} to Ni^{2+} concentration ratio. Fig.1C indicates that high density nanorods grow pointing to the center of the sphere. However, with further increasing reactant ratio, the precursors fail to grow dense thorns on their surface, and the existing thorns begin to fall from the spheres. When Co^{2+} to Ni^{2+} concentration ratio reaches 5∶1, the urchinlike structures decompose into the nanorod bundles and individual nanorods.

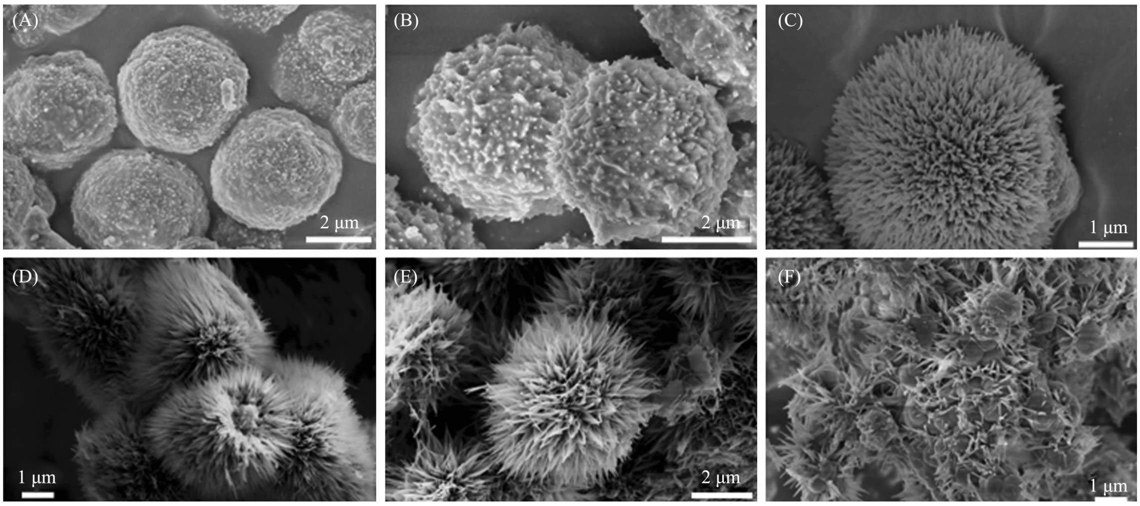

(A) Co^{2+}:Ni^{2+}=1∶2; (B) Co^{2+}:Ni^{2+}=1∶1; (C) Co^{2+}:Ni^{2+}=2∶1; (D) Co^{2+}:Ni^{2+}=3∶1; (E) Co^{2+}:Ni^{2+}=4∶1; (F) Co^{2+}:Ni^{2+}=5∶1

Fig.1 FE-SEM images of precursors with different concentration ratios of cobalt salt to nickel salt(T=75 ℃)

Fig.2 shows FE-SEM images of precursors at different reaction temperatures. As shown in Fig.2, the precursors are spherical particles with thorns radially distributed on the surface. The diameter and thorns length of the spherical precursor can be controlled by changing reaction temperature. With an increase in temperature, the diameters of spheres rise from 1.5~ 2.5 μm to 3~5 μm. The lengths of thorns are up to 0.6~1 μm when the reaction temperature is elevated to 90 ℃, as illustrated in Fig.2C. This indicates that a relatively higher temperature is advantageous to the formation of urchinlike micro/nano structures. Kinetics theory gives us an implication that the reaction temperature is an important factor in determining the rate of hydrolysis, nucleation as well as on the growth processes. The higher the temperature is, the more hydroxyl ions could be formed by hydrolyzation of urea, which favors the nucleation and growth of the precursors.

Moreover, it can be observed that the precipitator concentration causes some differences in the shapes of

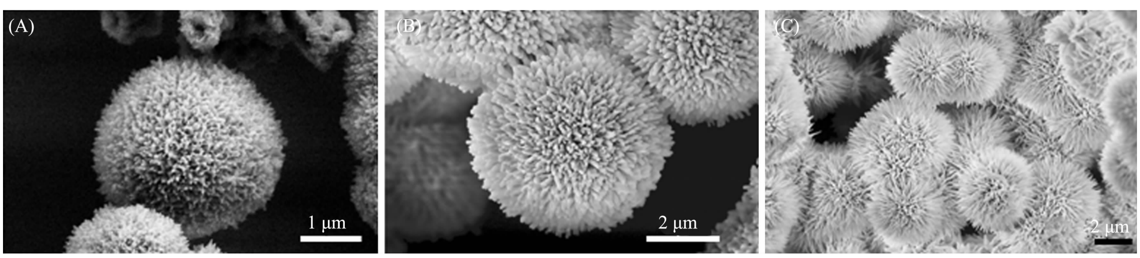

(A) 60 ℃; (B) 75 ℃; (C) 90 ℃

Fig.2 FE-SEM images of precursors at different reaction temperatures(Co^{2+}:Ni^{2+}=2∶1) precursors. Fig.3A, B depict the precursors are entirely spherical with clearly defined urchinlike micro/nano structure. By contrast, the thorns in Fig.3B are congregated more compactly into a sphere growing from the core. When the precipitator concentration is 30 times higher than the total concentration of Co^{2+} and Ni^{2+}, as is evident from Fig.3C, the obtained micro/nano structure is destroyed. The exposed core is composed of many irregular sheets. It can be deduced that the presence of an appropriate amount of urea plays a crucial role in the formation of urchinlike micro/nano structure.

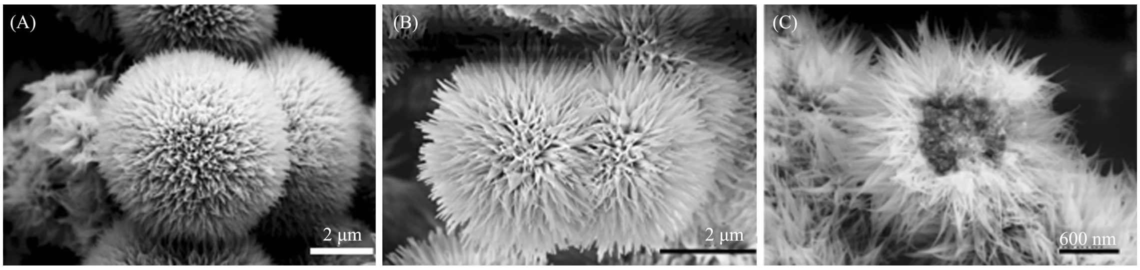

(A) 10 times, (B) 20 times, (C) 30 times than total of Co^{2+} and Ni^{2+}
T=90 ℃, Co^{2+}:Ni^{2+}=2:1

Fig.3　FE-SEM images of precursors with different precipitator concentrations

On the basis of the above results, we can conclude that the morphologies of the urchinlike precursors can be controlled by adjusting the particle growth rate which is a function of reaction temperature, reactant ratio of cobalt salt to nickel salt, and urea concentration. The formation of urchinlike particles is more favorable under the condition with the reaction temperature of 90 ℃, the molar ratio of Co^{2+} to $Ni^{2+}$of 2∶1, the precipitator concentration of 20 times higher than total concentration of Co^{2+} and Ni^{2+}. The diameter of spheres are between 2~5 μm, the thorns have a length of 500~800 nm with a tip diameter of 10~15 nm and a root diameter of 50~60 nm.

2.2　Heat treatment in oxidation atmosphere

Since the urchinlike precursors contain OH^- and massive adsorbed water, which leads to lattice expansion and poor thermal stability, they should be subjected to heat treatment in order to improve performances and stabilities. Taking the above optimal reaction system as an object, the powders heat-treated in oxidation atmosphere at 305 ℃ and 500 ℃(Fig.4A, B) inherit the morphologies of their precursors to some extent. Seen from the detailed structures of the inset TEM image of a single thorn, it demonstrates that these structures are built by many nanoparticles interconnected along the vertical direction of the core surface with an average size of 20 nm.

The precursors decompose to release H_2O and CO_2 when they are heated in oxidation atmosphere. The elimination of hydroxyl and carbonate groups from the precursors has great influence on the formation of new crystalline phase, thus resulting in the disruption of the original thorn-like morphology and leading to the architectures formed with nanoparticle array. The produced nanoparticles remain the relative positions along the patterns of their corresponding precursors[16].

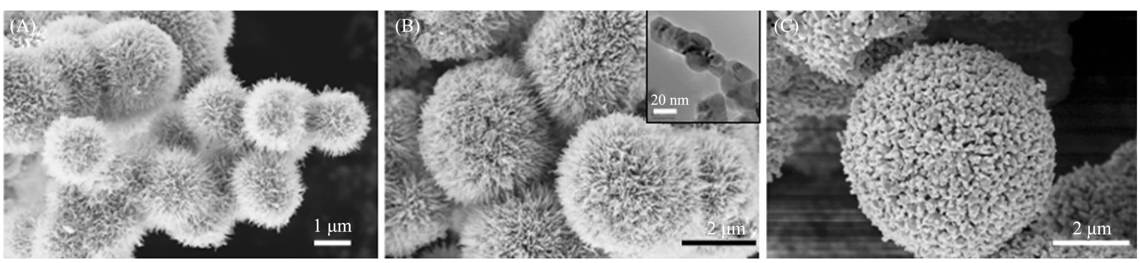

(A) 305 ℃; (B) 500 ℃, inset: TEM image of a single thorn; (C) 760 ℃
Precursors synthesis condition: T=90 ℃, Co^{2+}:Ni^{2+}=2:1

Fig.4　FE-SEM images of the precursor heat-treated at different temperatures in oxidation atmosphere

As the temperature elevates to 760 ℃, the morphology is quite different from the other two samples obtained at lower temperatures. The thorns begin to shorten and distribute randomly on the surface of spherical cores.

Fig.5 shows XRD patterns of the heat-treated powders obtained at different temperatures. It can be found that all of the main peaks are consistent with the characteristic peaks of $NiCo_2O_4$ (JCPDS file card, No. 20-781). When the temperature reaches 760 ℃, it is observed that the relatively pure phase $NiCo_2O_4$ decomposes into NiO and Co_3O_4.

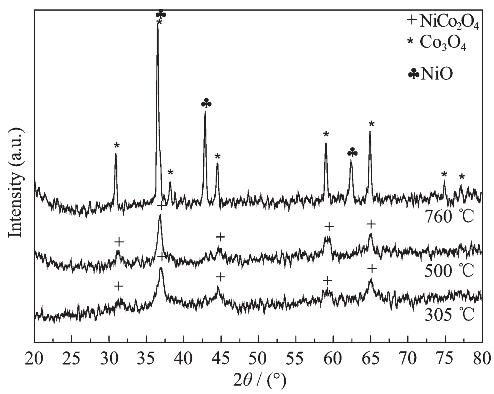

Fig.5 XRD patterns of heat-treated powders in oxidation atmosphere

The hysteresis loops results of heat-treated powders (expressed as T305, T500 and T760) are presented in Fig.6, which indicate that the powders exhibit the hysteresis loops of the ferrimagnetic nature at room temperature. The value of saturation magnetization(M_s) for T305(M_s=2.87 emu·g^{-1}) is larger than T500(M_s=2.32 emu·g^{-1}). Moreover, T500 exhibits significantly enhanced coercivity (H_c) (H_c =57 Oe) relative to T305(H_c=35.67 Oe). The improved magnetic property of T500 may be due to that the higher temperature is propitious to the main phase appearance.

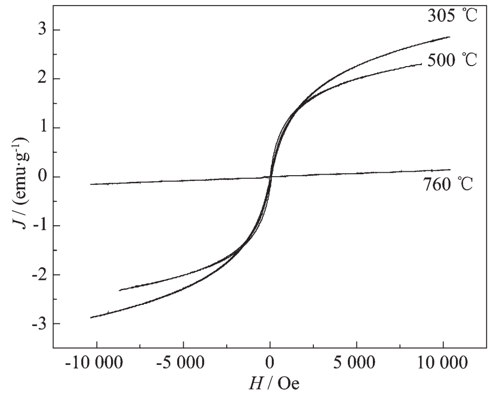

Fig.6 Magnetic hysteresis loops of heat-treated powders in oxidation atmosphere

The magnetic hysteresis loop of T760 is an oblique line which explains that the powders transform into superparamagnetism. This may be ascribed to $NiCo_2O_4$ absolutely decomposes into NiO and Co_3O_4 under this temperature. In addition, the magnetic properties are believed to be closely corresponded to product structures. With the temperature increasing, the ferrimagnetism of the prepared powders gradually weaken owing to the structure to be distorted, as shown in Fig.4C.

2.3 Heat treatment in reduction atmosphere

When these urchinlike precursors are reduced in reduction atmosphere, it can be seen clearly that there are comparatively huge differences between the resultant micro/nanospheres and their precursors as shown in Fig.7. Thorns forming the nanourchins grow into nanoparticles optionally piled up on the microspheres surface. It is known that the decomposition of precursors into NiO and Co_3O_4 may take place at 305 ℃ from XRD patterns as shown in Fig.8. As the temperature increases to 500 ℃, these

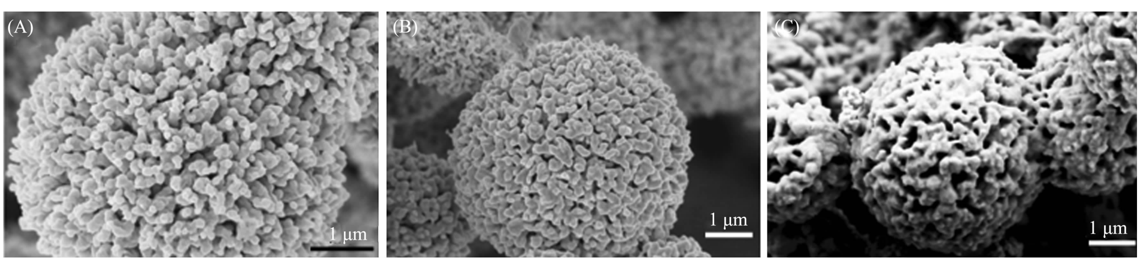

(A) 305 ℃; (B) 400 ℃; (C) 500 ℃

Precursors synthesis condition: T=80 ℃, Co^{2+}:Ni^{2+}=2:1

Fig.7 FE-SEM images of the precursor heat-treated at different temperatures in reduction atmosphere nanoparticles become smaller and mingle with the spheres. All diffraction peaks of the sample can be indexed with CoNi. The strong peaks and relatively low backgrounds reveal that the as-synthesized particles have a higher degree of crystallinity than particles treated at 400 ℃.

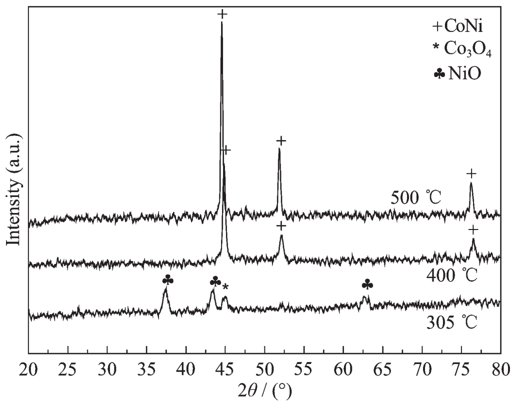

Fig.8　XRD patterns of heat-treated powders in reduction atmosphere

Fig.9 shows the coercivity and saturation magnetization heat-treated with different temperatures in reduction atmosphere. It illustrates that Hc and Ms of the loop increase with the synthesis temperature. Precursors formed antiferromagnetic NiO and Co_3O_4 in the reduction atmosphere at a lower temperature of 305 ℃. This is consistent with the result in the magnetic hysteresis loop. The H_c and M_s of particle obtained at 400 ℃ is 472.8 Oe and 97.54 emu·g^{-1}, whereas H_c is 235.7 Oe and M_s is 107.2 emu·g^{-1} at 500 ℃. According to the relationship among coercivity, saturation magnetization and crystal defects, microspheres at 500 ℃ possess improved crystallinity and less defects.

In addition, all the particles are ferrimagnetic and saturation magnetization is much higher compared to

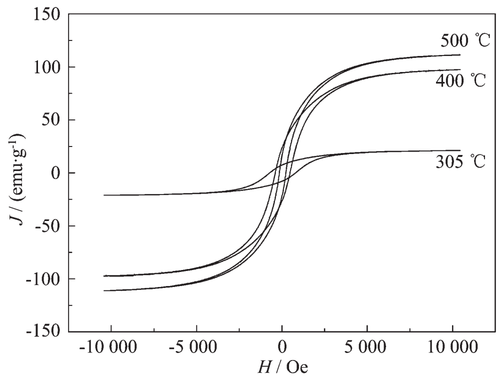

Fig.9　Magnetic hysteresis loops of heat-treated powders in reduction atmosphere

that at oxidation atmosphere (Fig.6). This is probably due to the increasing in the effective anisotropy of the heat-treated particles.

2.4 Possible growth mechanism of the urchinlike precursors

The TEM image (Fig.10A) shows several typical thorns growing from a core. When heat treated in oxidation atmosphere, it is interesting that the nanorods split into several nanoparticles which are orderly arranged into a line. The electron diffraction spots in the selected area electron diffraction (SAED) patterns (Fig.10C) separate clearly, which indicates these nanoparticles are well crystallized and self-assembled along a desired pattern. Experimental results suggest that the urchinlike particles may grow according to a "nucleation-growth-assembly" process. At the beginning of the reaction between cobalt salt, nickel salt and urea, the monomers nucleate and aggregate into spherical particles. When the reaction continues, the concentrations of these monomers in solution will continuously increase. They may serve as nuclei for the urchins to form similar thorn-shaped nanostructures on

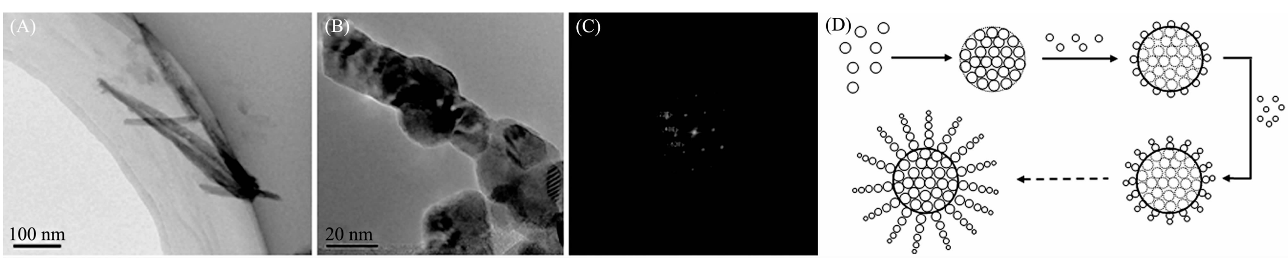

Fig.10　(A) TEM images of several typical nanorods in Fig.3B, inset: SAED from a single nanorod; (B) a amplied part of the nanorod inset in Fig.4B; (C) SAED from a single nanorod of (B); (D) The process of growing urchinlike micro/nano structures

the surface of spherical cores. The larger particles firstly deposit on the spheres surface, and the smaller particles will follow as the concentration of the reactants becomes lower. These nanoparticles have preferred orientation and link together along a particular growth direction as evidenced by the TEM image in Fig.10A. Extension of the reaction time results in the further growth of thorn-shaped structures, and urchinlike architectures are finally achieved[14].

3 Conclusions

In summary, we develop a mild, easily-controlled, and template-free method to prepare urchinlike micro/nano structured particles using urea as precipitants and nitrate as reacants. The characterization results demonstrate that the formation and properties of urchinlike structures could be influenced by various factors including reaction temperature, reactant concentration of metal salts and urea, heat-treated atmosphere and temperature. Under proper reaction conditions with the reaction temperature of 90 ℃, the molar ratio of Co^{2+} to Ni^{2+} of 2:1, the precipitator concentration of 20 times higher than total concentration of Co^{2+} and Ni^{2+}, well-defined urchinlike particles can be achieved with good ferrimagnetism.

References:

[1] Guilherme V M J, Alexandre G B, Paola C, et al. *J. Phys. Chem. C*, **2009**,**113**:7684-7691

[2] Hyeon T. *Chem. Commun.*, **2003**,**8**:927-934

[3] Mornet S, Vasseur S, Grasset F, et al. *Prog. Solid State Chem.*, **2006**,**34**:237-247

[4] Cao S W, Zhu Y J, Ma M Y, et al. *J. Phys. Chem. C*, **2008**, **112**:1851-1856

[5] Lee K R, Kim S, Kang D H, et al. *Chem. Mater.*, **2008**,**20**(21):6738-6742

[6] Lin X M, Samia A C S. *J. Magn. Magn. Mater.*, **2006**,**305**:100-109

[7] Lu A H, Salabas E L, Schüth F. *Angew. Chem. Int. Ed.*, **2007**,**46**(8):1222-1224

[8] Xiong S L, Xi B J, Qian Y T, et al. *Adv. Funct. Mater.*, **2007**,**17**:2728-2738

[9] Li H X, Bian Z F, Zhu J, et al. *J. Am. Chem. Soc.*, **2007**, **129**:8406-8407

[10]Umar A, Hahn Y B. *Cryst. Growth Des.*, **2008**,**8**(8):2741-2747

[11]Ung D, Viau G, Ricolleau C, et al. *Adv. Mater.*, **2005**,**17**(3):338-344

[12]Liu X H, Liang X D, Zhang N, et al. *Mater. Sci. Eng. B*, **2006**,**132**:272-277

[13]Liu X H, Zhang N, Yi R, et al. *Mater. Sci. Eng. B*, **2007**, **140**:38-43

[14]Ma F, Li Q, Li J G, et al. *J. Cryst. Growth*, **2008**,**310**:3522-3527

[15]WENG Ling-Yan(翁凌燕), LU Chun-Hua(陆春华), NI Ya-Ru(倪亚茹), et al. *Journal of Nanjing University of Technology: Natural Science Edition(Nanjing Gongye Daxue Xuebao: Ziran Kexue Ban)*, **2008**,**30**(6):63-66

[16]Li B X, Xie Y, Wu C Z, et al. *Mater. Chem. Phys.*, **2006**,**99**:479-486